Isotropic hyperfine splitting in the nitroxide radicals 4-amino-2,2,5,5-tetramethyl-3-imidazoline-*N*-oxyl and 4-amino-2,2,6,6-tetramethylpiperidine-*N*-oxyl

Larissa N. Ikryannikova,*[a] Leila Yu. Ustynyuk,[a] Boris V. Trubitsin,[b] Yurii A. Koksharov[b] and Alexander N. Tikhonov[b]

[a] *Department of Chemistry, M. V. Lomonosov Moscow State University, 119992 Moscow, Russian Federation. Fax: +7 095 939 4575; e-mail: larisa@kge.msu.ru*
[b] *Department of Physics, M. V. Lomonosov Moscow State University, 119992 Moscow, Russian Federation*

DOI: 10.1070/MC2004v014n05ABEH001910

Experimentally measured and DFT calculated isotropic hyperfine splitting constants for the nitroxide radicals 4-amino-2,2,5,5-tetramethyl-3-imidazoline-*N*-oxyl and 4-amino-2,2,6,6-tetramethylpiperidine-*N*-oxyl were compared to provide the basis for a choice of an appropriate level of low-cost DFT computations of electronic characteristics of nitroxide radicals.

Nitroxide radicals are widely used as spin probes for studying the structural and dynamic properties of biopolymers, membranes and different nanostructures.[1–4] The use of nitroxide radicals as spin probes is based on the sensitivity of their electron paramagnetic resonance (EPR) spectra to molecular mobility and environment (medium polarity, pH, microviscosity and ordering of solvent molecules). The development of quantum chemical approaches to adequate calculations of structural and electronic characteristics of nitroxide radicals is a topical problem of computational chemistry. The most informative EPR parameters of nitroxide radicals are the *g*-tensor and hyperfine splitting tensor, which are determined by the interaction of an unpaired electron with the nitrogen nucleus of the >N–O· fragment. Among spin labels, the nitroxide radicals 4-amino-2,2,5,5-tetramethyl-3-imidazoline-*N*-oxyl (ATI) and 4-amino-2,2,6,6-tetramethylpiperidine-*N*-oxyl (TA) are of special interest because they are often used as probes for measuring pH in different compartments of living cells[4–5] and heterogeneous chemical systems.[6] The EPR spectra of protonated and deprotonated ATI molecules are characterised by different hyperfine splitting constants; therefore, these species can be easily detected by EPR spectroscopy.

This work is aimed at the comparison of isotropic hyperfine splittings (a_{iso}) in nitroxide radicals ATI and TA, measured from their EPR spectra, with the a_{iso} constants calculated at different levels of density functional theory (DFT). Such a comparison is important for the development of appropriate approaches to efficient DFT calculations of EPR parameters of nitroxide radicals. It is known[7–12] that spin densities at nuclei, which determine the isotropic hyperfine splitting constant, are extremely sensitive to a choice of the computation method (exchange-correlation functional and basis set). Therefore, we compared experimental data with the a_{iso} computed at different levels of theory. All our calculations were performed for the nitroxide radicals in a gas phase. To the best of our knowledge, the gas phase constants a_{iso} for TA and ATI molecules are not available in the literature. To evaluate these constants, we measured the EPR spectra of TA and ATI dissolved in water-free organic solvents of different polarity (hexane, CCl_4, benzene, isopropanol and acetone) and water. The EPR spectra were measured on a Varian E-4 X-band spectrometer at 298 K. Spin label TA from Sigma was used, spin label ATI was a gift from Dr. I. A. Grigor'ev.

Figure 1(*a*) compares the EPR spectra of TA (at 298 K) dissolved in water or CCl_4, demonstrating a decrease in the hyperfine splitting constants a_{iso} in a non-polar solvent (CCl_4, $\varepsilon = 2.23$) as compared to water ($\varepsilon = 78.38$). Figure 2 shows the plots of measured a_{iso} versus solvent dielectric constant ε. For both radicals, TA and ATI, there is a correlation between the splitting constant a_{iso} and solvent polarity characterised by dielectric constant ε. In general, the parameter a_{iso} increases with ε. These results can be interpreted qualitatively in terms of the two main resonance structures >N–O· and >N$^+$–O$^-$, which differ with respect to the localisation of an unpaired electron either on the oxygen or nitrogen atom of the nitroxide fragment.

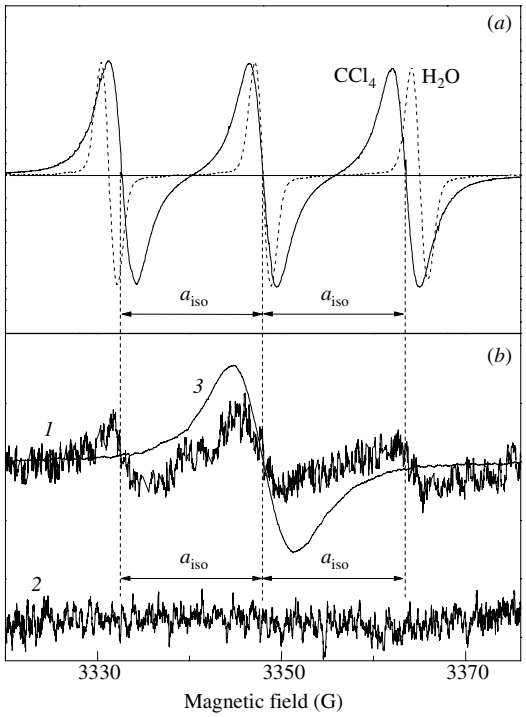

Figure 1 (*a*) Normalised EPR spectra of TA (0.1 mM) dissolved in water (dashed line) and CCl_4 (solid line). (*b*) EPR spectra of TA inside a quartz tube (internal diameter of 10 mm): (*1*) TA evaporated from a TA droplet by heating (≈ 350 K); a TA sample droplet was placed on the bottom of a closed quartz tube; (*2*) EPR signal recorded immediately after opening a tube cap; (*3*) TA in the bulk phase; this signal belongs to TA in the bulk phase (small droplets of TA accumulated on the tube walls). Microwave power, 1 mW; peak-to-peak modulation amplitude, 1 G.

A partial displacement of spin density from the O atom towards the N atom observed with the rise of solvent polarity is usually explained by stabilisation of the dipolar structure N$^+$–O$^-$ in polar surroundings. Stabilisation of the dipolar structure N$^+$–O$^-$ at the expense of the non-polar structure >N–O· reveals itself in the rise of parameter a_{iso}. However, there are specific interactions between a spin label and solvent molecules that can influence spin density partitioning in the nitroxide fragment. Actually, for spin labels dissolved in polar organic solvents characterised by similar dielectric constants, acetone ($\varepsilon = 20.74$) and isopropanol ($\varepsilon = 18.30$), the values of a_{iso} were markedly

Table 1 The examples of the basis sets B1 and B2 used in this work.

Basis set	Atoms	Orbital basis set	Auxiliary basis set
B1	C, O, N	(11*s*6*p*2*d*)/[6*s*3*p*2*d*]	(10*s*3*p*3*d*1*f*)
	H	(5*s*1*p*)/[3*s*1*p*]	(5*s*2*p*)
B2	C, O, N	(17*s*4*p*1*d*)/[3*s*2*p*1*d*]	(25*s*11*p*6*d*1*f*)/[4*s*3*p*2*d*1*f*]
	H	(8*s*1*p*)/[2*s*1*p*]	(8*s*1*p*)/[2*s*1*p*]

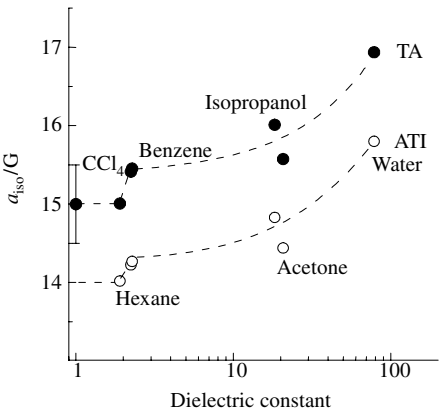

Figure 2 Spectral parameter a_{iso} of TA and ATI spin labels *versus* solvent dielectric constant.

different (Figure 2). For TA in acetone and isopropanol, we obtained a_{iso} = 15.57 (±0.02) and 16.01 (±0.02) G, respectively; for ATI in acetone and isopropanol, a_{iso} = 14.44 (±0.02) and 14.83 (±0.02) G, respectively. In case of non-polar solvents, CCl_4 (ε = 2.23) and benzene (ε = 2.27), the corresponding differences in hyperfine splitting constants were negligible (Figure 2).

We also attempted to measure the gas-phase splitting constants directly, by evaporating radicals from the droplets placed on the bottom of a closed EPR tube (below the EPR cavity). These measurements are complicated due to the low volatility of TA and ATI. However, we observed a weak triplet signal from TA [Figure 1(*b*), spectrum *1*], which can be attributed (at least partly) to radicals in the gas phase. This signal quickly disappeared after opening the EPR tube [Figure 1(*b*), spectrum *2*]. We suggest that the triplet signal can be attributed to either TA in gaseous surroundings or TA molecules adsorbed on the walls of the EPR tube. In the latter case, a surface concentration of TA is not high enough to cause a transformation of the triplet spectrum to a single line. Figure 1(*b*) (spectrum *1*) allows us to characterise weakly interacting molecules of TA by $a_{iso} \approx$ $\approx$ 15±0.5 G, which is the same (within experimental error) as the hyperfine splitting constant of TA in hexane (a_{iso} = 15 G). A broadening of the triplet lines [Figure 1(*b*), spectrum *1*] can be caused by TA interactions with oxygen inside a closed tube. Batchellor[13] also mentioned that EPR signals in polyatomic species in gases are complicated by a broadening of the EPR spectra due to the spin–rotation interaction. Note that an obvious asymmetry of the triplet indicates that the central line might be contaminated by a singlet line from the bulk-phase species [Figure 1(*b*), spectrum *3*], which differs from a triplet signal assigned to the gas-phase TA. For ATI, we failed to detect a gas-phase-like EPR signal. However, it is reasonable to suggest that the isotropic hyperfine constant for the gas phase ATI has approximately the same value as ATI in hexane, *i.e.*, $a_{iso} \approx$ 14 G (Figure 2).

Table 2 Calculated isotropic hyperfine splitting constants (a_{iso}) and spin densities on the atom (σ_N).

Theory level	a_{iso}/G		σ_N (a.u.)	
	TA	ATI	TA	ATI
PBE/B1	10.1	7.0	0.39	0.40
PBE/B2//B1	13.8	10.6	0.39	0.39
BLYP/B2//B1	14.1	11.2	0.39	0.39
B3LYP/B1	11.0	7.7	0.48	0.44
B3LYP/6-21G	17.2	15.7	0.40	0.40
B3LYP/6-31G	15.1	13.2	0.44	0.44
B3LYP/6-31G*	13.8	11.2	0.44	0.44
B3LYP/6-31G**	13.9	11.2	0.44	0.44
B3LYP/6-311G	9.6	7.5	0.44	0.45
B3LYP/EPR-II	12.3	9.8	0.45	0.46
EPR (in hexane)	15.0±0.2	14.0±0.2	—	—
EPR (gas phase)	15.0±0.5	—	—	—

All calculations were performed for deprotonated forms of TA and ATI using the PRIRODA program developed by Laikov[14] or the standard GAUSSIAN98 package.[13] In case of the PRIRODA program, we optimised a spin label geometry using the PBE or BLYP functionals and basis sets B1. To determine the hyperfine coupling constant a_{iso}, we performed single-point computations with the use of the basis set B2 (Table 1). Computations with the functional B3LYP were carried out with the use of the GAUSSIAN98 package and a standard basis set (Table 2). To verify the calculation methods used, we have compared geometry parameters (bond lengths, angles and torsions) calculated for the spin label 4-hydroxy-2,2,6,6-tetramethylpiperidine-*N*-oxyl (TEMPOL), which is similar to TA, with published data on the crystal structure of TEMPOL.[7] The results of our calculations for TEMPOL are consistent with experimental data. Note that, in both cases, TA and ATI, the calculations of geometry parameters performed at different levels of theory (Table 2, left column) gave practically the same results.

The isotropic hyperfine coupling constant a_{iso}, which measures the Fermi contact interaction between the unpaired electron and the nitrogen nucleus of the >N–O$^{\cdot}$ fragment, was calculated as

$$a_{iso} = \frac{8}{3}\pi g_e \beta_e g_n \beta_n \rho(\bar{r}_N), \quad (1)$$

where $\rho(\bar{r}_N)$ represents the electron spin density at the nitrogen nucleus, g_e is the free-electron *g*-factor, β_e is the Bohr magneton, g_n and β_n are the nuclear *g*-factor and nucleus magneton, respectively. The results of a_{iso} calculations for the gas phase TA and ATI are given in Table 2. We obtained a rather significant scattering of a_{iso}, whose values depended on the computation level. For TA, the calculation at the levels PBE/B2//B1, BLYP/B2//B1, B3LYP/6-31G, B3LYP/6-31G* and B3LYP/6-31G** gave the values of a_{iso} close to the experimental value $a_{iso} \approx$ 15 G. Other approaches led to underestimated (PBE/B1, B3LYP/B1, B3LYP/6-311G and B3LYP/EPR-II) or overestimated (B3LYP/6-21G) constants. For ATI, a reasonable result was obtained only at the B3LYP/6-31G level of computations, while the other methods (except for B3LYP/6-21G) gave underestimated a_{iso} values. Note that the B3LYP/6-31G level of calculations provides the best results for both of the spin labels. For TA, this approach gives a slightly overestimated result, contrary to an underestimated a_{iso} value for ATI. These results demonstrate that an accurate calculation of the splitting constant a_{iso} strongly depends on the calculation level because some of the methods overestimate spin density at the N nucleus of the nitroxide radical, while the other give underestimated values. Note that, contrary to calculated spin densities at the nitrogen nucleus, which determines the Fermi contact spin-nuclear interaction, spin densities on the nitrogen atoms (Table 2, parameter σ_N) are much less sensitive to the computation level. One might expect that further amendments (*i.e.*, corrections for radical vibrations[10] or the use of more sophisticated *ab initio* methods[11]) could provide more accurate results in the computations of EPR parameters of nitroxide radicals.

In summary, we conclude that in case of the functional B3LYP the use of the basis set 6-31G provided the best results. The use of the functionals PBE and BLYP with the basis set B2 incorporated into the PRIRODA[12] package also gave reasonable results. Note that the main advantage of the PRIRODA program is that it allows relatively fast DFT calculations to be performed for large molecular systems without losses of computation accuracy. This opens perspectives for DFT computations of the EPR parameters of nitroxide radicals in different chemical and biochemical systems, *i.e.*, spin labels surrounded by different solvents.[12] We hope that further progress in computational chemistry will help to overcome the problem of accurate calculations of the EPR parameters of spin labels.

We are grateful to Dr. V. A. Chertkov for his help in the quantum chemical calculations with the GAUSSIAN98 program suite and to Professor V. V. Lunin for fruitful discussions. This

study was supported by INTAS (grant nos. 99-1086, 01-483 and 03-55-1436), the Russian Foundation for Basic Research (grant no. 03-04-48981) and the 'Russian Universities' Foundation (grant no. 01.03.081).

References

1 *Spin Labeling: Theory and Applications*, ed. L. J. Berliner, Academic Press, New York, 1976.

2 *Biological Magnetic Resonance*, eds. L. J. Berliner and J. Reuben, Plenum, New York, 1989, vol. 8.

3 V. V. Kramtsov and L. B. Volodarsky, in *Biological Magnetic Resonance*, Plenum, New York, 1998, vol. 14.

4 A. N. Tikhonov and W. K. Subczynski, in *Biological Magnetic Resonance*, eds. S. S. Eaton, G. R. Eaton and L. J. Berliner, Kluwer, New York, 2004, vol. 23, p. 147.

5 B. V. Trubitsin and A. N. Tikhonov, *J. Magn. Reson.*, 2003, **163**, 257.

6 E. V. Lunina, *Appl. Spectrosc.*, 1996, **50**, 1413.

7 V. Barone, A. Bencini, M. Cossi, A. di Matteo, M. Mattesini and F. Totti, *J. Am. Chem. Soc.*, 1998, **120**, 7069.

8 A. Zakrassov and M. Kaftory, *J. Solid State Chem.*, 2002, **169**, 75.

9 W. Koch and M. C. Holthousen, *A Chemist's Guide to Density Functional Theory*, Viley-VCH Verlag GmbH, Germany, 2001.

10 R. Improta, G. Scalmani and V. Barone, *Chem. Phys. Lett.*, 2001, **336**, 349.

11 M. Kaupp, in *EPR Spectroscopy of Free Radicals in Solids. Trends in Methods and Applications*, eds. A. Lund and M. Shiotani, Kluwer, Dordrecht, 2003.

12 L. N. Ikryannikova, L. Yu. Ustynyuk and A. N. Tikhonov, *J. Phys. Chem. A*, 2004, **108**, 4759.

13 S. N. Batchelor, *Chem. Phys. Lett.*, 1998, **288**, 119.

14 D. Laikov, *Chem. Phys. Lett.*, 1997, **281**, 151.

15 M. J. Frisch, G. W. Trucks, H. B. Schlegel, G. E. Scuseria, M. A. Robb, J. R. Cheeseman, V. G. Zakrzewski, J. A. Montgomery, Jr., R. E. Stratmann, J. C. Burant, S. Dapprich, J. M. Millam, A. D. Daniels, K. N. Kudin, M. C. Strain, O. Farkas, J. Tomasi, V. Barone, M. Cossi, R. Cammi, B. Mennucci, C. Pomelli, C. Adamo, S. Clifford, J. Ochterski, G. A. Petersson, P. Y. Ayala, Q. Cui, K. Morokuma, P. Salvador, J. J. Dannenberg, D. K. Malick, A. D. Rabuck, K. Raghavachari, J. B. Foresman, J. Cioslowski, J. V. Ortiz, A. G. Baboul, B. B. Stefanov, G. Liu, A. Liashenko, P. Piskorz, I. Komaromi, R. Gomperts, R. L. Martin, D. J. Fox, T. Keith, M. A. Al-Laham, C. Y. Peng, A. Nanayakkara, M. Challacombe, P. M. W. Gill, B. Jonson, W. Chen, M. W. Wong, J. L. Andres, C. Gonzalez, M. Head-Gordon, E. S. Replogle and J. A. Pople, *Gaussian98, Revision A.11*, Gaussian, Inc., Pittsburgh, PA, 2001.

Received: 24th February 2004; Com. 04/2236